Chemical Physics Letters 610–611 (2014) 70–75

Contents lists available at ScienceDirect

Chemical Physics Letters

journal homepage: www.elsevier.com/locate/cplett

Heterogeneous reaction of particulate chlorpyrifos with NO_3 radicals: Products, pathways, and kinetics

Nana Li, Peng Zhang, Bo Yang, Jinian Shu*, Youfeng Wang, Wanqi Sun

Research Center for Eco-Environmental Sciences, Chinese Academy of Sciences, Beijing 100085, China

ARTICLE INFO

Article history:
Received 12 May 2014
In final form 27 June 2014
Available online 8 July 2014

ABSTRACT

Chlorpyrifos is a typical chlorinated organophosphorus pesticide. The heterogeneous reaction of chlorpyrifos particles with NO_3 radicals was investigated using a vacuum ultraviolet photoionization aerosol time-of-flight mass spectrometer (VUV-ATOFMS) and a real-time atmospheric gas analysis mass spectrometer. Chlorpyrifos oxon, 3,5,6-trichloro-2-pyridinol, *O*,*O*-diethyl *O*-hydrogen phosphorothioate, *O*,*O*-diethyl ester thiophosphoric acid, diethyl hydrogen phosphate and a phosphinyl disulfide compound were identified as the main degradation products. The heterogeneous reaction pathways were proposed and their kinetic processes were investigated via a mixed-phase relative rate method. The observed effective rate constant is $3.4 \pm 0.2 \times 10^{-12}$ cm^3 molecule^{-1} s^{-1}.

1. Introduction

Chlorpyrifos, *O*,*O*-diethyl-*O*-(3,5,6-trichloro-2-pyridyl) (Figure 1), a member of phosphorothioate class of chlorinated organophosphorus compounds, is a moderately toxic broad-spectrum pesticide [1]. It is widely applied in agriculture [1–4], animal houses [5], and in the control of household pests, such as subterranean termites [2,6,7]. Chlorpyrifos inhibits acetylcholinesterase activity and protein synthesis and affects the functions of cells, axons, and brain [7]. Long-term exposure to low levels of chlorpyrifos can lead to impaired neurobehavioral performance [8]. Chlorpyrifos has been used as a model compound to forecast the environmental fate of organophosphorothioate pesticides (OP) under drinking water chlorinated treatment conditions [9]. Extensive researches have been conducted on the chlorpyrifos' detection methods, toxic effects [1], transformation, and degradation processes of chlorpyrifos in water and soil [9,10]. It was reported that atmosphere is a major receptacle and transport medium for pesticides through their spraying, volatilization, or wind erosion of soil particles and dusts which are loaded with pesticides [11–16]. Chlorpyrifos is a potential long-range transport pesticide in the atmosphere [17]. Therefore, a comprehensive knowledge of chlorpyrifos' behavior in the atmosphere is necessary to understand its environmental impact.

Many studies have been conducted on transformations of chlorpyrifos under different physical, chemical, and biological conditions. Raymond et al. studied the degradation of chlorpyrifos in soil from a cranberry bog [10]. 3,5,6-Trichloro-2-pyridinol (TCP) and chlorpyrifos oxon were assigned as the main degradation products of chlorpyrifos [10]. The attenuation of chlorpyrifos by the enriched indigenous soil microorganism was studied in aqueous and soil slurry environments by Tiwari et al. [18]. They identified the anaerobic and aerobic degradation pathways of chlorpyrifos, including oxidation and hydrolysis [18]. Stephene Duirk et al. investigated the degradation of chlorpyrifos in aqueous chlorine solutions and found that chlorpyrifos oxon and TCP were the main oxidation products [9]. TCP was also identified as the fungal degradation product by K. Maya et al. [6]. Zhang et al. investigated the degradation of chlorpyrifos in aqueous solution by ultrasonic irradiation and found that chlorpyrifos oxon and TCP were also generated from pyrolysis reactions of chlorpyrifos in water during ultrasonic irradiation [19]. In the atmosphere, chlorpyrifos oxon was identified as the main degradation of chlorpyrifos [17]. In a word, chlorpyrifos oxon and TCP are two primary transformation products of chlorpyrifos, which are derived from the oxidation of the P═S double bond into the P═O bond and hydrolysis at the P—O bond adjacent to the benzene ring, respectively. Although many researches have been conducted on the degradation of chlorpyrifos by photolysis [3,20], hydrolysis [10], and microorganisms [21], most of them have focused on the transformations of chlorpyrifos in soil and water. Chlorpyrifos can exist in both gas and particle phases in the ambient atmosphere because of its semi-volatile nature (1.8×10^{-5} mm Hg at 25 °C) [22–25]. Borrás et al. reported that the concentrations of particulate and gaseous chlorpyrifos range in 0.22–2.66 and 29.10–1428.28 ng m^{-3}, respectively, in the atmosphere after pesticide application [23]. However, the

* Corresponding author.
E-mail address: jshu@rcees.ac.cn (J. Shu).

http://dx.doi.org/10.1016/j.cplett.2014.06.062
0009-2614/

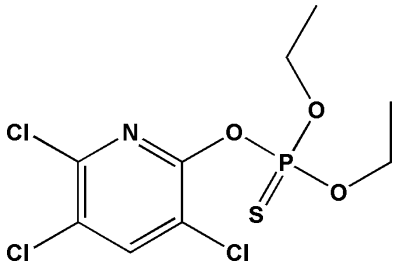

Figure 1. Chemical structure of chlorpyrifos.

chemical transformations of chlorpyrifos, especially for particulate chlorpyrifos, in the atmosphere are not well understood.

Chemical transformations of pesticides in the atmosphere occur mainly through photolysis and reaction with atmospheric oxidants such as hydroxyl radicals (OH), ozone (O_3), and nitrate radicals (NO_3) [26–28]. NO_3 radicals are present in the atmosphere at a low concentration during the day because they are highly photolytic, but they can rapidly accumulate to an appreciable concentration at night. Thus, NO_3 radicals play an important role in the nighttime atmosphere and affect the transformations of atmospheric organic pollutants. In this study, the heterogeneous oxidation of chlorpyrifos particles by NO_3 radicals is investigated with the use of a vacuum ultraviolet photoionization aerosol time-of-flight mass spectrometer (VUV-ATOFMS) and an online atmospheric gas analysis mass spectrometer. The reaction products are obtained, the heterogeneous reaction pathways are proposed, and the effective rate constant is measured. The experimental results contribute in understanding the atmospheric transformations of chlorpyrifos at night.

2. Experimental

2.1. Chemicals

Chlorpyrifos (Sigma–Aldrich, 99.9%), P_2O_5 (Sinopharm Chemical Reagent Co., Ltd., 98%), azelaic acid (NRSCRD, China, 99%), nitrogen (Beijing Huayuan Gas Chemical Industry Co., Ltd., 99.99%), dichloromethane (J. T. Baker Co., Chromatographic grade), isoprene (Alfa Aesar, 99%), absolute ethyl alcohol (Sinopharm Chemical Reagent Co., Ltd., 99.7%), and fuming nitric acid (Beijing Lisui Chemical Factory, 95%) were used in the experiment.

2.2. Preparation of NO_3 radicals

NO_3 radicals were generated by thermal decomposition of N_2O_5 placed at the room temperature ($N_2O_5 \Leftrightarrow NO_2 + NO_3$) [29]. N_2O_5 was synthesized by dehydrating concentrated nitric acid ($2HNO_3 \Leftrightarrow N_2O_5 + H_2O$). The P_2O_5 powder was slowly added into a wide-mouth glass bottle containing fuming nitric acid (30 ± 1 mL) at 220 ± 2 K. At the same time, the mixture was stirred continuously with a glass rod until it turned into uniform mixture. The mixture was then heated in a water bath controlled by a thermostatic oven at 313 K and the N_2O_5 was collected into a 1000 mL flask kept in a liquid nitrogen trap. Prior to N_2O_5 collection, the brown gas NO_2 that volatilized from the fuming nitric acid in flask was removed by a pump at a temperature of 243 ± 2 K.

2.3. Experimental setup

The experimental setup of the heterogeneous reaction of chlorpyrifos aerosols with NO_3 radicals has been described in detail in literature [30]. In summary, it consists of an aerosol generator, a reaction chamber, and online analytical instruments.

The aerosol generator was an electric tube furnace comprising two tandem quartz tubes (50 cm (length) × 3 cm (inner diameter)), which are equipped with independent temperature controllers. The chlorpyrifos aerosols were generated by the homogeneous nucleation method. Azelaic acid was used to produce nuclei because of its limited reactivity with NO_3 radicals. Azelaic acid (0.15 g) was placed in the first tube (433 ± 2 K), in which nuclei were generated through high-temperature evaporation and condensation. Chlorpyrifos was placed in the second tube (413 ± 2 K), where the gaseous chlorpyrifos then could be coated on the azelaic acid particles. A N_2 stream flowed through both of the quartz tubes at 0.6 L min^{-1} sequentially and introduced the chlorpyrifos-coated azelaic acid particles into the reaction chamber. A scanning mobility particle sizer (SMPS, TSI 3081) was used to monitor the mass concentration of the chlorpyrifos particles. The particles produced in the experiment were polydisperse: the geometric mean diameters of the azelaic acid particles and the chlorpyrifos-coated ones were 245.7 ± 5 and 282.1 ± 9 nm, respectively. The thickness of the chlorpyrifos shell is roughly estimated to be ~20 nm and the mass concentration of the chlorpyrifos particles is ~577 μg m^{-3}.

The reaction chamber consisted of a ~180 L thin-walled open head stainless steel drum sealed with a collapsible Teflon bag. The air was filtered by activated carbon, silica gel, and absorbent cotton before entering the reaction chamber. The experiments were conducted under atmospheric pressure at room temperature of ~288 K. The average relative humidity in the chamber is measured to be ~40% by a vaisala humicap (HMM 100). A magnetic-driven fan was placed at the bottom during the reaction to ensure that the reactants were mixed rapidly and sufficiently. When the signal value of chlorpyrifos particles reached about 3000 counts/10 s, isoprene (30 μL) was injected into the chamber as the reference compound to estimate the concentration of NO_3 radicals. The initial concentration of isoprene in the chamber was $1.0 \pm 0.2 \times 10^{15}$ molecules cm^{-3}, measured using an online atmospheric gas analysis mass spectrometer (QIC-20-HAL3F-RC, Hiden) via detection of the mass peak at m/z 67 ($C_5H_7^+$). When the signal of m/z 67 stabilizes, N_2O_5 was brought into the reaction chamber continuously by a N_2 stream at a volumetric flow rate of 0.6 L min^{-1}.

The concentration and chemical composition of particles in the reaction chamber were monitored real-time with a laboratory-built VUV-ATOFMS which has been described in detail in literature [31]. An 8 mm diameter copper rod coupled with a cartridge heater placed in the detection chamber was used to vaporize the particles, and the nascent organic vapor was photoionized with light radiated from a laboratory-assembled VUV lamp powered by RF of 80 W [32]. The ions produced by VUV photoionization were extracted into a field-free flight distance of 1.4 m by an ion optical system and then detected by a microchannel plate detector.

2.4. Gas chromatography and mass spectrometry (GC–MS)

After completion of the heterogeneous reaction, the particles in the reactor were captured by a sampler equipped with an ultra-fine glass fiber filter. The filter covered with particles was then placed in 5 mL dichloromethane and ultrasonically washed for 3 min. The extract solution was analyzed with GC–MS immediately to identify the reaction products. The GC–MS (Agilent 6890) is equipped with a 30 m × 0.25 mm × 0.25 μm HP-5 capillary column and an HP-5973 quadrupole mass filter with a 70 eV electron impact ionizer. The temperature of the capillary column was set at 60 °C for 1 min then increased to 220 °C at a rate of 20 °C min^{-1} and held for 8 min.

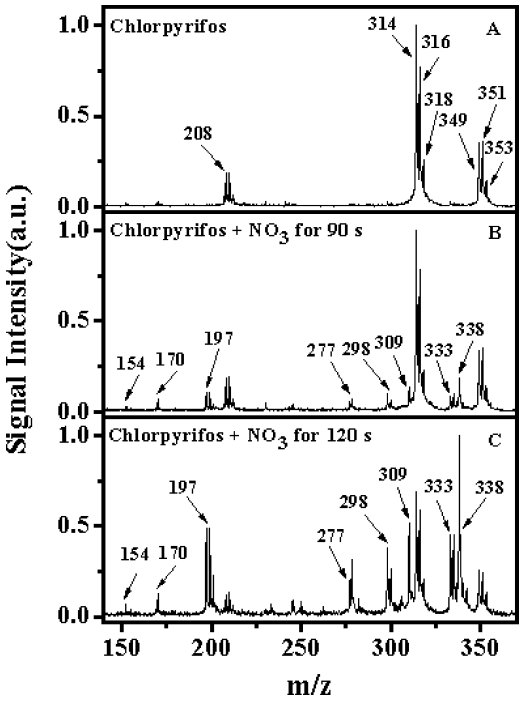

Figure 2. Time-of-flight mass spectra of chlorpyrifos particles (A) and its reaction products by exposing to NO_3 radicals for 90 s (B) and 120 s (C).

3. Results and discussion

Aside from NO_3 radicals, NO_2 was also generated during the thermal decomposition process of N_2O_5. The reactivity between chlorpyrifos and NO_2 was evaluated by exposing the chlorpyrifos particles to NO_2 at a concentration of $3.5 \pm 0.3 \times 10^{14}$ molecules cm^{-3} for 15 min. No apparent product signal was detected by the online ATOFMS. Since the average total duration of the experiments is ~170 s, the direct reaction between NO_2 and the chlorpyrifos particles was neglected. In addition, no apparent reaction product was detected by ATOFMS when pure azelaic acid particles exposed to NO_3 radicals at a concentration of $5.0 \pm 0.3 \times 10^{10}$ molecules cm^{-3} for 20 min. In this experiment, the effect of reaction between azelaic acid and NO_3 radicals was also negligible.

3.1. Heterogeneous reaction products

The TOF mass spectra of chlorpyrifos particles and their heterogeneous reaction products are shown in Figure 2A–C. The spectra were acquired at 0, 90, and 120 s after the particles were exposed to NO_3 radicals. The acquisition time for each mass spectrum was 10 s and each mass spectrum was normalized to its most intense mass peak. The mass peaks at *m/z* 349, 351, and 353 in Figure 2A are assigned to the molecular ions of chlorpyrifos with isotopic combinations of $^{35}Cl_3$, $^{35}Cl_2{}^{37}Cl$, and $^{35}Cl^{37}Cl_2$ [33], respectively. These peak intensities are consistent with the natural isotope abundances of the chlorine atom. The mass peaks at *m/z* 314, 316, and 318 are attributed to daughter ions of chlorpyrifos after losing a Cl atom during the VUV photoionization. The degradation products can also exhibit a cluster of peaks because of the isotopic ions. Thus, to facilitate analysis, the first peak of the cluster is selected to represent the compound in this study. The mass peak at *m/z* 208 can be attributed to impurities in sample or detection system.

Compared with Figure 2A, the new mass peaks at *m/z* 154, 170, 197, 277, 298, 309, 333, and 338 arise and increase gradually after the particles were exposed to NO_3 radicals, as shown in Figure 2B and C. These mass peaks are attributed the oxidation products of chlorpyrifos. Given that the mass peaks at *m/z* 154, 170, 277, 309, and 338 are not accompanied with cluster peaks similar to those for the molecular ions of chlorpyrifos, we speculate that the ions with these mass peaks do not contain chlorine atoms. By comparison, the ions at *m/z* 197, 298, and 333 are speculated to contain chlorine atoms based on the obvious isotope peaks around them. The mass peak at *m/z* 333 is assigned to the molecular ion of chlorpyrifos oxon (PI). Chlorpyrifos oxon is a typical oxidation product of chlorpyrifos under atmospheric conditions [34]. The mass peak at *m/z* 298 is the daughter ion of PI after losing one ^{35}Cl atom during the VUV photoionization. The mass peak at *m/z* 197 is assigned as 3,5,6-trichloro-2-pyridinol (TCP, PII), a product observed previously in the hydrolysis of chlorpyrifos [19]. Chlorpyrifos oxon and TCP were identified as degradation products of both ozonolysis and OH-oxidation experiments of particulate chlorpyrifos [35]. The mass peak at *m/z* 170 may be O,O-diethyl O-hydrogen phosphorothioate (PIII) and/or O,O-diethyl ester thiophosphoric acid (PIV) in the TOF mass spectra. The peak at *m/z* 154 is assigned to be diethyl hydrogen phosphate (PV), which is the oxidation product of PIII. The highest mass peak at *m/z* 338 in Figure 2C is assigned as a disulfide compound (PVI) on the basis of its molecular weight and the characteristic peak. Since the mass peaks at *m/z* 309 and 277 exhibit isolated single peak shape similar to the peak of PVI, as well as peak intensities that change with the signal strength of PVI, we speculate that they are contributed from the daughter ions of PVI after losing an ethyl and subsequently subtracting two oxygen atoms or one sulphur atom, respectively, during the VUV photoionization.

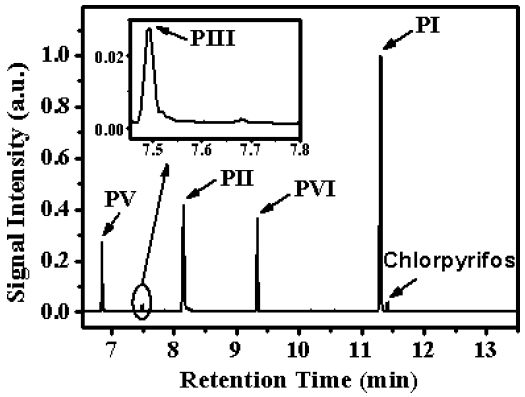

Figure 3. GC–MS total ion chromatography (TIC) of chlorpyrifos particles and its reaction products.

Chlorpyrifos is a moderately toxic broad-spectrum pesticide. However, the toxicities of its degradation products can be even stronger. The oxygen analog (P=O) of organophosphorus pesticides has more effective toxicity than its thiophosphoryl function (P=S) [36], thus the potential risks of chlorpyrifos oxon (PI) to human health might be severer than its parent chemical (chlorpyrifos). It was reported that the 3,5,6-trichloro-2-pyridinol (TCP, PII) exhibits low-to-moderate toxicity to invertebrates, fish, birds, and mammals based on acute toxicity tests [5]. Therefore, the risks of TCP to human health also cannot be ignored.

The total ion chromatography (TIC) of chlorpyrifos and its heterogeneous reaction products are shown in Figure 3. The products PV ($C_4H_{11}O_4P$, mol. wt. 154), PIII ($C_4H_{11}O_3PS$, mol. wt. 170), PII ($C_5H_2ONCl_3$, mol. wt. 197), PI ($C_9H_{11}O_4NPCl_3$, mol. wt. 333), and chlorpyrifos appeared at the retention times of 6.84, 7.49, 8.16, 11.30, and 11.42 min, respectively. The compound PIV ($C_4H_{11}O_3PS$, mol. wt. 170) possessing the same mass peak than PIII in the TOF mass spectra was not detected by GC–MS, which may be due to the thiol compounds' chemical polarity and thermal instability [37]. PVI was also not confirmed successfully because a standard mass

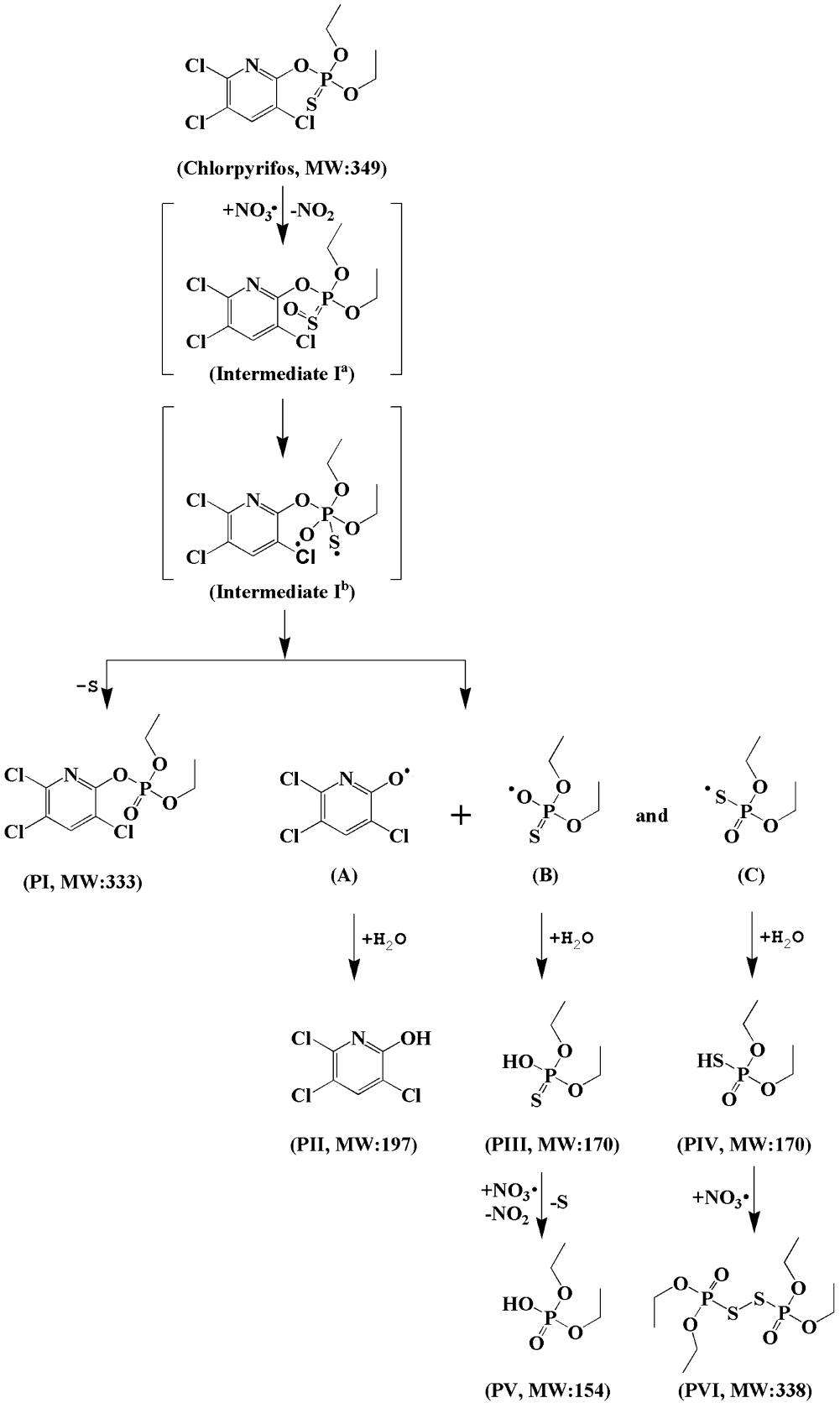

Figure 4. Proposed reaction pathways for the heterogeneous reaction of particulate chlorpyrifos with NO_3 radicals.

spectrum is unavailable in the NIST library. We speculate that the compound with a retention time at 9.33 min may be the product PVI ($C_8H_{20}O_6P_2S_2$, mol. wt. 338) because its main characteristic peaks at m/z 113, 141, 170, 202 in the electron ionization mass spectra do not contain chlorine atoms. This speculation is consistent with the obtained TOF mass spectra. Some discrepancies may exist between the degradation products of chlorpyrifos in this study and those in wastewater and in aqueous suspensions [3], which may be due

to the different degradation conditions such as light, catalyst, and electrolysis.

3.2. Reaction pathways

Based on the observed products, the proposed reaction pathways for the heterogeneous reaction of chlorpyrifos particles with NO_3 radicals are shown in Figure 4. The P=S double bond is the most reactive group in the chlorpyrifos molecule. The NO_3 radicals attack the chlorpyrifos molecule by attaching an oxygen atom on the sulfur atom, giving the intermediate I^a. The attachment of an oxygen atom is speculated to be formed by addition of NO_3 radicals, followed by a loss of a NO_2 molecule [29]. The intermediate I^a then rearranges, leading to the formation of the diradical intermediate I^b [32]. One evolution of I^b involves the transformation of the P=S double bond into the P=O double bond. And PI forms via the loss of a sulfur atom of intermediate I^b. The transformation of the P=S double bond into the P=O double bond is a common degradation pathway for organophosphorus pesticide, whether in soil, water, or atmospheric environment [10,38,39]. Another pathway may begin with the cleavage of the P–O bridge bond connecting the benzene ring of intermediate I^b, resulting in the generation of the reactive substances A, B, and C (radicals). Subsequently, the reactive substance A converts to PII in the presence of water. In this study, hydrolysis and oxidation are two transformation mechanisms for the reactive substances B and C in this study. The hydrogenation of substance B results in the generation of PIII, which is further oxidized into PV. The oxidation mechanism could be similar to the transformation from chlorpyrifos to PI. The reactive substance C undergoes hydrolyzation to yield a thiol compound (PIV), which is then further oxidized into a phosphinyl disulfide compound (PVI) by NO_3 radicals. The PIII and PIV are also observed in the reaction between chlorpyrifos-methyl with OH radicals [38]. The proposed formation mechanism of the disulfide compound is in accordance with the previous reports on the phosphinyl disulfides formed from thiols [33,37,40]. The similar disulfide compounds have also been observed in the heterogeneous reaction of suspended malathion particles with NO_3 radicals and ozone in previous studies [33,41]. Some differences are found between the proposed pathways in this study and those of chlorpyrifos in aqueous solution by ultrasonic irradiation and in a cranberry bog by soil microorganism [10,19]. In the aqueous solution media by ultrasonic irradiation and the natural cranberry bog media, only PI and PII were observed as the degradation products of chlorpyrifos. Whereas, PIII, PIV, PV, and PVI along with PI and PII were observed in our experiments. Thus the corresponding reaction pathways were more than that in other media, which can due to the discrepancies of degradation environments.

3.3. Effective rate constant

A mixed-phase relative rate method is used to estimate the effective reaction rate of chlorpyrifos particles with NO_3 radicals because the concentration of NO_3 radicals is difficult to measure directly in the reaction. Isoprene is selected as the gas-phase reference material because its reaction rate constant of gas-phase isoprene with NO_3 radicals is considered to be a constant value in this study. The attenuation of gas-phase reference material, isoprene, can be expressed by the following Eq. (1) [42].

$$\ln\left(C^{g}_{ref}/C^{g}_{ref0}\right) = -k^{g}_{ref}\overline{C^{g}_{NO_3}}\,t \quad (1)$$

where C^{g}_{ref0} and C^{g}_{ref} are the initial and real-time concentrations of gas-phase isoprene, respectively, k^{g}_{ref} is the gas-phase reaction rate constant of isoprene with NO_3 radicals ($7.0 \pm 0.2 \times 10^{-13}$ cm^3 molecule^{-1} s^{-1} at 298 K) [43], $\overline{C^{g}_{NO_3}}$ represents the average concentration of NO_3 radicals in the chamber, and t is the reaction time.

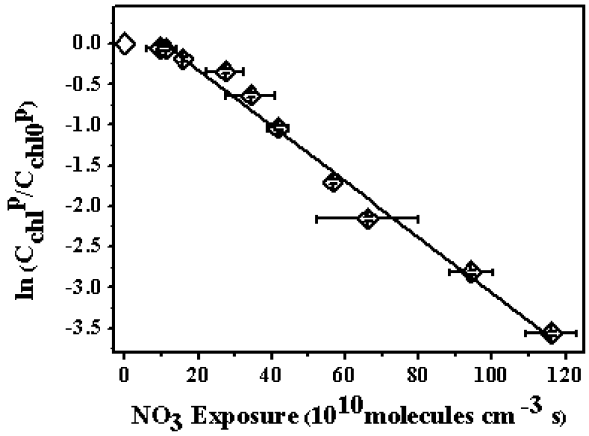

Figure 5. Plots of $\ln\left(C^{p}_{chl}/C^{p}_{chl0}\right)$ versus $\overline{C^{g}_{NO_3}}\,t$ for the reaction of particulate chlorpyrifos with NO_3 radicals.

By plotting $-\ln\left(C^{g}_{ref}/C^{g}_{ref0}\right)$ versus $k^{g}_{ref}t$, the slope of linear regression represents $\overline{C^{g}_{NO_3}}$. The calculated values of $\overline{C^{g}_{NO_3}}$ is $9.9 \pm 0.3 \times 10^{10}$ molecule cm^{-3}.

The decay rate of chlorpyrifos particles with NO_3 radicals can be calculated using Eq. (2) [44]:

$$\ln\left(C^{p}_{chl}/C^{p}_{chl0}\right) = \left(k^{p}_{chl}\right)_{eff}\left[\frac{\ln\left(C^{g}_{ref}/C^{g}_{ref0}\right)}{k^{g}_{ref}}\right] \quad (2)$$

Here, C^{p}_{chl0} and C^{p}_{chl} are the initial and real-time concentrations of chlorpyrifos particles, respectively, and $\left(k^{p}_{chl}\right)_{eff}$ represents the effective reaction rate constant of particulate chlorpyrifos with NO_3 radicals.

Combining Eq. (1) with Eq. (2), Eq. (3) can be derived as following:

$$\ln\left(C^{p}_{chl}/C^{p}_{chl0}\right) = -\left(k^{p}_{chl}\right)_{eff}\overline{C^{g}_{NO_3}}\,t \quad (3)$$

Therefore, by plotting $\ln\left(C^{p}_{chl}/C^{p}_{chl0}\right)$ versus $\overline{C^{g}_{NO_3}}\,t$ in Figure 5, the effective rate constant $\left(k^{p}_{chl}\right)_{eff}$ can be obtained.

Since the total wall losses the particulate chlorpyrifos was less than 0.05, it was neglected in the data process. This may result in overestimating the value of the rate constant at a certain extent. Figure 5 shows the plots of the measured $\ln\left(C^{p}_{chl}/C^{p}_{chl0}\right)$ versus $\overline{C^{g}_{NO_3}}\,t$ for chlorpyrifos. Error bars represent the standard deviations of the three duplicate experiments. The plot shown in Figure 5 fits well with the linear least-squares fitting ($R^2 > 0.96$). The slope of linear regression represents the effective reaction rate constant $\left(k^{p}_{chl}\right)_{eff}$ for the reaction of chlorpyrifos particles with NO_3 radicals, which is $3.4 \pm 0.2 \times 10^{-12}$ cm^3 molecule^{-1} s^{-1}. A. Muñoz et al. reported that the value of the OH reaction rate constant with gas-phase chlorpyrifos is $9.1 \pm 2.1 \times 10^{-11}$ cm^3 molecule^{-1} s^{-1} (303 ± 5 K) [34], which is slightly faster than the reaction rate of chlorpyrifos particles with NO_3 radicals. It should be noted that in our studies the reaction rate constant may be overestimated due to the volatility of particulate chlorpyrifos during reaction process. Besides, since the pesticide was coated in the suspended nano-sized aerosols in our experiments, the heterogeneous reaction rate constant obtained might be greater than that adsorbed on agglomerated silica or silicon dioxide particles. In the real atmosphere, aerosols have more complex factors such as physical morphologies, air humidity, and

illumination intensity affecting the effective reaction of chlorpyrifos particles with NO_3 radicals. Consequently, discrepancies may exist in the effective reaction rate constant of chlorpyrifos particles between the smog chamber in our laboratory and the real atmosphere.

The tropospheric lifetime of particle-phase chlorpyrifos at lower tropospheric concentration of NO_3 radicals at night (5×10^8 molecules cm^{-3}) [45] is estimated to be 9.8 min ($\tau = 1/(k^p_{chl})_{eff}[NO_3]$). However, the lifetime of atmospheric chlorpyrifos particles may be much longer than 9.8 min. The thickness of real chlorpyrifos aerosols is roughly at the micrometer level, which is far larger than the thickness of chlorpyrifos particles (~20 nm) in the experiment. The lifetimes of gas-phase chlorpyrifos toward OH radicals and O_3 are approximately 2 and 10 h, respectively [34] which are much longer than the lifetime of chlorpyrifos particles toward NO_3 radicals observed in the experiment. Even the lifetime of atmospheric chlorpyrifos particle may vary according to its morphology and atmospheric circumstance, this experimental results reveal that heterogeneous reaction with NO_3 radicals is an important degradation method for chlorpyrifos in the atmosphere.

4. Conclusion

The reaction products of chlorpyrifos particles with NO_3 radicals have been obtained using a smog chamber coupled with online ATOFMS and off-line GC–MS. Chlorpyrifos oxon, 3,5,6-trichloro-2-pyridinol, O,O-diethyl O-hydrogen phosphorothioate, O,O-diethyl ester thiophosphoric acid, diethyl hydrogen phosphate and one kind of phosphinyl disulfides are the six degradation products observed in the heterogeneous NO_3 oxidation of chlorpyrifos particles. One reaction pathway is the transformation of the P=S double bond into the P=O double bond, which is similar to the heterogeneous reaction mechanism of many organothiophosphorus pesticides with NO_3 radicals [29,33,41]. Hydrolysis plays a vital part in the heterogeneous reaction of chlorpyrifos particles with NO_3 radicals. Products II, III, and IV were all generated via hydrolysis reaction. The obtained effective rate constant of chlorpyrifos particles with NO_3 radicals is $3.4 \pm 0.2 \times 10^{-12}$ cm^3 $molecule^{-1}$ s^{-1}. The lifetime of chlorpyrifos particles is ~9.8 min. The results reveal that NO_3 radicals play an important role in the degradation of chlorpyrifos in ambient air. These experimental results may shed light on the chemical behavior of chlorpyrifos particles and its analogs in the atmosphere.

Acknowledgments

This research is funded by National Natural Science Foundation of China (Grant No. 21277155 and 21207143).

References

[1] K. Maya, R. Singh, S. Upadhyay, S.K. Dubey, Process Biochem. 46 (2011) 2130.
[2] G. Briceño, M. Fuentes, G. Palma, M. Jorquera, M. Amoroso, M. Diez, Int. Biodeterior. Biodegradation 73 (2012) 1.
[3] V.G.G. Kanmoni, S. Daniel, G.A.G. Raj, React. Kinet. Mech. Cat. 106 (2012) 325.
[4] K.D. Racke, K.P. Steele, R.N. Yoder, W.A. Dick, E. Avidov, J. Agric. Food Chem. 44 (1996) 1582.
[5] S. Baskaran, R.S. Kookana, R. Naidu, Aust. J. Soil Res. 41 (2003) 749.
[6] K. Maya, S. Upadhyay, R. Singh, S.K. Dubey, Bioresour. Technol. 126 (2012) 216.
[7] G. Tortella, O. Rubilar, M. Castillo, M. Cea, R. Mella-Herrera, M. Diez, Chemosphere 88 (2012) 224.
[8] J.D. Sherman, Arch. Environ. Health 51 (1996) 5.
[9] S.E. Duirk, T.W. Collette, Environ. Sci. Technol. 40 (2006) 546.
[10] R.A. Putnam, J.O. Nelson, J.M. Clark, J. Agric. Food Chem. 51 (2003) 170.
[11] L.S. Aston, J.N. Seiber, J. Environ. Qual. 26 (1997) 1483.
[12] M.S. Majewski, M.M. McChesney, J.E. Woodrow, J.H. Prueger, J.N. Seiber, J. Environ. Qual. 24 (1995) 742.
[13] R. Risebrough, R. Huggett, J.t. Griffin, E. Goldberg, Science 159 (1968) 1233.
[14] H.F. Van Dijk, R. Guicherit, Water Air Soil Pollut. 115 (1999) 21.
[15] A. Wolters, V. Linnemann, M. Herbst, M. Klein, A. Schäffer, H. Vereecken, J. Environ. Qual. 32 (2003) 1183.
[16] B. Yang, Y. Zhang, J. Meng, J. Gan, J. Shu, Environ. Sci. Technol. 44 (2010) 3311.
[17] D. Mackay, J.P. Giesy, K.R. Solomon, Ecological Risk Assessment for Chlorpyrifos in Terrestrial and Aquatic Systems in the United States, vol. 231, 2014, pp. 3.
[18] M.K. Tiwari, S. Guha, Water Res. 51 (2014) 73.
[19] Y. Zhang, Y. Hou, F. Chen, Z. Xiao, J. Zhang, X. Hu, Chemosphere 82 (2011) 1109.
[20] M. Ismail, H.M. Khan, M. Sayed, W.J. Cooper, Chemosphere 93 (2013) 645.
[21] L.G. Sultatos, M. Shao, S. Murphy, Toxicol. Appl. Pharmacol. 73 (1984) 60.
[22] R. Bailey, W. Belzer, J. Agric. Food Chem. 55 (2007) 1150.
[23] E. Borrás, P. Sánchez, A. Muñoz, L. Tortajada-Genaro, Anal. Chim. Acta 699 (2011) 57.
[24] E. Hart, C. Coscollà, A. Pastor, V. Yusà, Atmos. Environ. 62 (2012) 118.
[25] Z. Chishti, S. Hussain, K.R. Arshad, A. Khalid, M. Arshad, J. Environ. Manage. 114 (2013) 372.
[26] R. Atkinson, R. Guicherit, R.A. Hites, W.-U. Palm, J.N. Seiber, P. De Voogt, Water Air Soil Pollut. 115 (1999) 219.
[27] M.J. Al Rashidi, A. Chakir, E. Roth, J. Phys. Chem. A 117 (2013) 2908.
[28] C. Liu, J. Gan, Y. Zhang, M. Liang, X. Shu, J. Shu, B. Yang, J. Phys. Chem. A 115 (2011) 10744.
[29] I. Wangberg, I. Barnes, K.H. Becker, Environ. Sci. Technol. 31 (1997) 2130.
[30] Y. Zhang, B. Yang, J. Meng, S. Gao, X. Dong, J. Shu, Atmos. Environ. 44 (2010) 697.
[31] J. Shu, S. Gao, Y. Li, Aerosol Sci. Technol. 42 (2008) 110.
[32] Y. Wang, B. Yang, P. Zhang, W. Zhang, C. Liu, X. Shu, J. Shu, J. Phys. Chem. A 116 (2012) 10802.
[33] J. Meng, B. Yang, Y. Zhang, X. Dong, J. Shu, Chemosphere 79 (2010) 394.
[34] A. Muñoz, M. Ródenas, E. Borrás, M. Vázquez, T. Vera, Chemosphere 111 (2014) 522.
[35] A. El Masri, M. Al Rashidi, H. Laversin, A. Chakir, E. Roth, RSC Adv. (2014), http://dx.doi.org/10.1039/C4RA03511A.
[36] D. Yan, X. Jiang, S. Xu, L. Wang, Y. Bian, G. Yu, Chemosphere 71 (2008) 1809.
[37] E.M. Bellet, J.E. Casida, J. Agric. Food Chem. 22 (1974) 207.
[38] A. Muñoz, et al., Environ. Sci. Technol. 45 (2011) 1880.
[39] Y. Samet, L. Agengui, R. Abdelhédi, Chem. Eng. J. 161 (2010) 167.
[40] T. Miyamoto, I. Yamamoto, J. Pestic. Sci. 2 (1977) 303.
[41] C. Liu, B. Yang, J. Gan, Y. Zhang, M. Liang, X. Shu, J. Shu, Chemosphere 87 (2012) 470.
[42] J. Smith, et al., Atmos. Chem. Phys. 9 (2009) 3209.
[43] Evaluated Kinetic Data. www.iupac-kinetic.ch.cam.ac.uk
[44] K.E. Huff Hartz, E.A. Weitkamp, A.M. Sage, N.M. Donahue, A.L. Robinson, J. Geophys. Res. Atmos. 112 (2007) D04204.
[45] R. Atkinson, J. Phys. Chem. Ref. Data 20 (1991) 459.